UNIVERSITY OF LEEDS

This is a repository copy of *Engine Hot Spots: Modes of Auto-ignition and Reaction Propagation*.

White Rose Research Online URL for this paper:
http://eprints.whiterose.ac.uk/93443/

Version: Accepted Version

Article:
Bates, L, Bradley, D, Paczko, G et al. (1 more author) (2016) Engine Hot Spots: Modes of Auto-ignition and Reaction Propagation. Combustion and Flame, 166. pp. 80-85. ISSN 0010-2180

https://doi.org/10.1016/j.combustflame.2016.01.002

© 2016. This manuscript version is made available under the CC-BY-NC-ND 4.0 license
http://creativecommons.org/licenses/by-nc-nd/4.0/

Reuse
Unless indicated otherwise, fulltext items are protected by copyright with all rights reserved. The copyright exception in section 29 of the Copyright, Designs and Patents Act 1988 allows the making of a single copy solely for the purpose of non-commercial research or private study within the limits of fair dealing. The publisher or other rights-holder may allow further reproduction and re-use of this version - refer to the White Rose Research Online record for this item. Where records identify the publisher as the copyright holder, users can verify any specific terms of use on the publisher's website.

Takedown
If you consider content in White Rose Research Online to be in breach of UK law, please notify us by emailing eprints@whiterose.ac.uk including the URL of the record and the reason for the withdrawal request.

White Rose university consortium
Universities of Leeds, Sheffield & York

eprints@whiterose.ac.uk
https://eprints.whiterose.ac.uk/

Engine Hot Spots: Modes of Auto-ignition and Reaction Propagation

L. Bates[a], D. Bradley[a*], G. Paczko[b], N. Peters[b]
[a]School of Mechanical Engineering, University of Leeds, UK, [b] Institute for Combustion Technology, RWTH Aachen, Germany.

*Corresponding author

E-mail address: d.bradley@leeds.ac.uk

Keywords:

Ignition delay time, Excitation time, Hot spots, Detonation Peninsula, Auto-ignitive propagation, Super-knock.

Abstract

Many direct numerical simulations of spherical hot spot auto-ignitions, with different fuels, have identified different auto-ignitive regimes. These range from benign auto-ignition, with pressure waves of small amplitude, to super-knock with the generation of damaging over-pressures. Results of such simulations are generalised diagrammatically, by plotting boundary values of ξ, the ratio of acoustic to auto-ignition velocity, against ε. This latter parameter is the residence time of the developing acoustic wave in the hot spot of radius r_o, namely r_o/a, normalised by the excitation time for the chemical heat release, τ_e. This ratio controls the energy transfer into the developing acoustic front. A third relevant parameter involves the product of the activation temperature, *E/R*, for the auto-ignition delay time, τ_i, normalised by the mixture temperature. *T*, the ratio, τ_i / τ_e, and the dimensionless hot spot temperature gradient, $\left(\partial \ln T/\partial \bar{r}\right)$, where $\bar{r}$ is a dimensionless radius. These parameters define the boundaries of regimes of thermal explosion, subsonic auto-ignition, developing detonations, and non-auto-ignitive deflagrations, in plots of ξ against ε.The regime of developing detonation forms a peninsula and contours, throughout the field. The product parameter $\left(E/RT\right)\left(\tau_i/\tau_e\right)/\partial \ln T/\partial \bar{r}$ expresses the influences of hot spot temperature gradient and fuel characteristics, and a unique value of it might serve as a boundary between auto-ignitive and deflagrative regimes. Other combustion regimes can also be identified, including a mixed regime of both auto-ignitive and "normal"

deflagrative burning. The paper explores the performances of a number of different engines in the regimes of controlled auto-ignition, normal combustion, combustion with mild knock and, ultimately, super-knock. The possible origins of hot spots are discussed and it is shown that the dissipation of turbulent energy alone is unlikely to lead directly to sufficiently energetic hot pots. The knocking characterisation of fuels also is discussed.

1. Introduction

Reactive hot spots can arise for a number of reasons: partial mixing with hot gas or burned products, heat transfer from hot surfaces, and turbulent energy dissipation in flowing reactants. Their size may be of the order of millimetres. Following Zel'dovich [1], a gradient of reactivity can give rise to an auto-ignition velocity, u_a. At one extreme this can lead to a detonation, at another, to a benign, controlled auto-ignitive propagation. The rate of change of the heat release rate at the hot spot determines the associated amplitude of the generated pressure pulse and, if u_a is high enough, to be close to the acoustic speed, a, this pulse can be coupled with the heat release in a detonation wave.

Earlier findings [2,3] from direct numerical simulations, DNS, of hot spot auto-ignitions in 0.5 H_2/0.5 CO/air mixtures showed a peninsula could be constructed, within which detonations could develop. The boundaries were defined by the dimensionless groups, a/u_a, and $r_o/a\tau_e$, in which r_o is the radius of a spherical hot spot and τ_e is the excitation time. This is the time during which most of the heat release occurs at the end of the auto-ignition delay time, τ_i [4].

This approach has been employed in studies of engine knock and super-knock in gasoline engines [5-10]. The phenomena leading to super-knock are a rather complex sequence of events comprising the primary formation of hot spots that pre-ignite and initiate premature flame propagation, with earlier increases in pressure and temperature in the unburned mixture. A secondary, more reactive, hot spot may then be generated in the reactants and lead to a developing detonation, following the theory developed in [2,3]. While the salient features of the latter appear to be understood, the mechanisms causing the primary hot spots are still the subject of debate. The earlier the initial pre-igniton, the more severe is the secondary auto-ignition. The cyclical nature of "super-knock" is discussed in Section 5. The paper focuses on the secondary hot spots and the parameter range within which a detonation can develop. The original simulations have been extended to other fuels and focus on the secondary hot spots, by relating the detonation peninsula also to the auto-ignitive activation energy of the mixture and hot spot temperature gradient. This extended understanding is able to characterise engine auto-ignition over a wide range of conditions from benign auto-ignition, through mild knock, to super-knock and offers a fundamental approach to assessing the anti-knock characteristics of fuels.

2. Auto-ignition in the strong ignition regime

The auto-ignition delay time at a given pressure is expressed by :

$$\tau_i = Cexp(E/RT), \text{ and} \quad (1)$$

$$\partial\tau_i/\partial T = \tau_i\left(E/RT^2\right). \quad (2)$$

The localised auto-ignitive activation temperature, *E/R*, is expressed by:

$$\partial \ln \tau_i/\partial(1/T) = E/R. \quad (3)$$

Assuming that the reactivity gradients arise solely from changes in temperature with the radius, *r*, the auto-ignition propagation velocity is

$$u_a = \partial r/\partial\tau_i = (\partial r/\partial T)(\partial T/\partial\tau_i). \quad (4)$$

Detonations are associated with the auto-ignitive front propagating at close to the acoustic velocity, *a*, and it is convenient to introduce the dimensionless ratio, ξ:

$$\xi = a/u_a = (\partial T/\partial r)(\partial\tau_i/\partial T)a. \quad (5)$$

The way in which ξ decreases with increasing temperature is shown for the Primary Reference Fuels, *i*-octane/*n*-heptane, in Fig. 1, for five different Octane Numbers, and an assumed value of $(\partial T/\partial r)$ of -2K/mm. The data on τ_i are from [11], and the values of *a* are from [12]. Between about 700 and 800K there is a sharp decrease in $(\partial\tau_i/\partial T)$ with *T* and, consequently, also in ξ. This is countered in the regime of negative temperature coefficient, but is subsequently resumed at about 1000K, as ξ approaches unity. In the absence of a negative temperature coefficient, the same temperature gradient that can ignite a detonation at a high temperature, quenches it at a lower temperature, as noted in [13].

A critical value of the temperature gradient, signified by suffix *c*, occurs when ξ = 1.0, and from Eq. (5),

$$(\partial T/\partial r)_c = (\partial T/a\partial\tau_i). \quad (6)$$

From Eqs (5) and (6),

$$\xi = (\partial T/\partial r)(\partial T/\partial r)_c^{-1}. \quad (7)$$

For a given mixture and its conditions, ξ is proportional to $\partial T/\partial r$.

From Eqs. (2) and (5),

$$\xi = -\tau_i\left(E/RT^2\right)(\partial T/\partial r)a. \quad (8)$$

Both Voevodsky and Soloukhin [14], and Meyer and Oppenheim [15], employing H_2/O_2 mixtures, used Eq. (2) to define the boundary between strong and weak auto-ignitions. Strong ignition was defined as a stable detonation, with near-instantaneous and uniform auto-ignition, and a low value of $\left(\partial\tau_i/\partial T\right)$. Meyer and Oppenheim suggested a threshold value of $\partial\tau_i/\partial T$ for this regime of - 2 μs/K.

Figure 2 shows results from the DNS studies of [2,3], for a detonation developing rapidly from a hot spot of radius 3 mm, in a stoichiometric mixture of 0.5 H_2/0.5 CO/air, with ξ = 1.0 at 1200K, τ_i = 39.16 μs, and a = 731 m/s. The Chapman-Jouguet wave speed is soon attained within the hot spot. The temperature gradient across the hot spot was -2.426 K/mm, and the value of $\partial\tau_i/\partial T$ was -0.564 μs/K, is smaller than the value of Meyer and Oppenheim. A hot spot developing into a thermal explosion was also investigated in [2,3] with ϕ = 0.75 and at 1000K. This showed a value of $\partial\tau_i/\partial T$ of -32 μs/K. Similar plots of hot spot histories for other conditions appear in [2,3].

3. Excitation time and the detonation peninsula

This features the other relevant dimensionless group formulated in [2,3]. The nature of an auto-ignition also depends upon the rate at which the heat is released at the end of the delay time [4,13]. The time for the acoustic wave to move through the hot spot of radius r_o, divided by the excitation time, τ_e, is defined by ε:

$$\varepsilon = r_o/a\tau_e \,. \tag{9}$$

It is a measure of the energy transferred into the acoustic front: the acoustic wave transit time through the hot spot, divided by the time for the heat release.

From Eq. (8)

$$\xi = -\left(\tau_i\, E/RT\right)\left(\partial T/T/\partial r/r_O\right)a/r_O \,. \tag{10}$$

Introducing τ_e, gives

$$\xi\varepsilon = -\bar{E}\left(\partial \ln T/\partial \bar{r}\right), \text{ where} \tag{11}$$

$$\bar{E} = \frac{\tau_i}{\tau_e}\frac{E}{RT} \text{ and } \bar{r} = r/r_o \,.$$

If T_o is peak temperature at the centre of the hot spot, $\partial \ln T/\partial \bar{r}$ can be approximated by ln(T/T_o). The associated error for an assumed constant linear gradient, $\partial T/\partial r$, ranges from 0.05% for $\partial T/\partial r$ = -1 K/mm, to 4.7% for -100 K/mm. Little is known of the detailed structure of hot spots, but various

DNS studies of turbulent flow suggest a structure less ordered than the spherical geometry envisaged here. Essentially r_o can be regarded as the length over which the temperature gradient is nearly constant.

In a different context, Lee, Radulsecu, Sharpe, Shepherd and co-workers [16-19] have demonstrated the importance of $\overline{E}$ in assessing the stability of detonations. Low values of both *E/RT* and τ_i/τ_e are conducive to a spatially more uniform reaction zone, more strongly coupled with the shock wave. These terms are related to ξ and ε in Eq. (11), through the driving hot spot temperature gradient [6,20]. Higher values of *E/R* make oblique detonations more unstable, creating an irregular cellular structure [21].

Figure 3 shows plots of ξ against ε that define the peninsula within which detonations can develop from hot spot auto-ignitions, as well as the extent of other auto-ignition regimes. The peninsula, defined by its upper and lower limits of ξ_u and ξ_l, was constructed from the results of many simulations of separate hot spot auto-ignitions. The absence of turbulence was not unduly restrictive, as turbulence time scales can be about three orders of magnitude larger than the auto-ignition times. If a hotspot initiates a propagating flame, initially it will be laminar, with progressively increased wrinkling, length scales, and acceleration due to turbulence as it propagates [22]. As ε is increased, more of the heat release is transferred into the acoustic front, to extend the range of ξ values that can support a developing detonation, as can be seen from the figure. This aspect is demonstrated by the simulation shown in Fig. 4 of [3], in which the developing strength of the acoustic front can be observed as it moves outwards, and develops into a detonation outside the hot spot.

The original simulations involved H_2/CO/air mixtures [2,3], chosen because the detailed chemical kinetics were well established. Additional data for *n*-heptane/air and *i*-octane/air mixtures were subsequently simulated by Peters and Paczko. The original data centred around values of $\overline{E}$ of (110 ± 67).10^3 at 1100K, and (15.6 ± 8).10^3 at 1000K for H_2 /CO. The later values were 2.45.10^3 at 800K for *n*-heptane and 58.7.10^3 at 893K for *i*-octane. Although the different values of $\overline{E}$ have but small influence upon the detonation peninsula boundaries, they influence the hot spot temperature elevation, through Eq. (11). If $\overline{E}$ is known, the value of $\partial \ln T/\partial \overline{r}$ then might be found at any point. It is, however, difficult to designate values of $\partial \ln T/\partial \overline{r}$, for reasons discussed in Section 6.

The full line curves defining the peninsula in Fig. 3 are best fit curves for these different sources of data. Within the important narrow toe of the peninsula developing detonations are confined to the lower values of ξ, approaching unity. The lower values of ξ_u and the narrowing of the toe at the small values of ε arise because insufficient of the heat release is transferred into the developing

acoustic wave. Thermal explosions, at values of ξ below ξ_l, are more rapid, with less severe pressure fronts than those in Fig. 2, and temperature gradients that are smaller [2,3].

4. Onset of deflagration

Above the upper limit, ξ_u, of the developing detonation peninsula, the ensuing propagation of reaction after hot spot auto-ignition becomes increasingly deflagrative as ξ increases. Further auto-ignition is, of course, not precluded outside the peninsula, but the pressure pulses will be relatively weak, with no transition to detonation.

The DNS of Sankaran et al. of turbulent homogeneous mixtures [23] explored the regime within which deflagrative and auto-ignitve propagations co-exist. These simulations showed that when $\partial T/\partial r$ is small, auto-ignitive propagation speeds are high in relation to those of laminar flames but, as this gradient is increased, a transition to a slower reaction front occurs, with a deflagration speed that is controlled by molecular transport processes. Initially, about 17% of the heat release rate was from deflagrative flames and the remainder from auto-ignitive propagation. This suggests that the hot spot critical radii were attained for both modes of continuing propagation, but that the auto-ignitive ones were dominant. The smaller and more stretched kernels did not develop, while the larger ones survived. A transition parameter, β, was defined in [23] as the deflagration velocity, u_d, normalised by u_a. With $\beta > 1$, the deflagration front became dominant, although, initially, the deflagration velocity would not be fully developed.

Following earlier studies of *i*-octane auto-ignition [24], Mansfield and Wooldridge [25] found that, with a 0.59 H_2/0.41 CO/N_2/air syngas mixture, at ϕ = 0.5, β became greater than unity at $\partial T/\partial r$ ~ -5 K/mm. With this gradient, an assumed hot spot radius, r_o, of 3 mm, and $\overline{E}$ = 110. 10^3 at 1100K, $\overline{E}\left(\partial \ln T/\partial \overline{r}\right)$ = 1490. The generalised relationship for this parameter = 1500 is shown in Fig. 3, as a tentative threshold for the onset of a deflagration. Usually, there is no sharp division between auto-ignitive and deflagrative propagation, and this is clear from the DNS of [23] and [26], which reveal a broad regime in which the two modes co-exist.

The dominance of the auto-ignitive mode, $\beta < 1$, involved additional criteria and these can arise in two contrasting ways, which are independent of u_a. The first is when u_d, is either a laminar or a turbulent burning velocity, significantly less than u_a. The second occurs when, with increasing turbulence, u_d, and β, after attaining a peak value with $\beta > 1$, then decline, due to the onset of localised flame extinctions arising from the increasing flame stretch rate, with $\beta = 0$ at complete flame quench. This regime, discussed in Section 6, is identified in [27,28]. It has been shown to be suitable

for controlled auto-ignitive engine combustion in [29]. Practical engine combustion in such mixed regimes is now discussed in Section 5.

5. Engine performance and the detonation peninsula

Following the earlier employment of the detonation peninsula [5-10], it has been used in a combined experimental engine and LES study to demonstrate how increasing spark advance, and the associated increasingly severe engine knock, cause the corresponding engine cycle loci to cross the threshold into the detonation peninsula [30].

Lean-burn engine combustion is efficient and reduces pollutant emissions, but improved performance is curtailed by the lean flammability limits under turbulent conditions and low burning velocities. These limitations can be overcome with auto-ignitive propagation [31]. This requires high temperature to enhance auto-ignitive burning, and lean mixtures with low O_2 content, and recirculated exhaust gas to reduce deflagrative flame propagation. Such a regime has been variously defined as one of controlled auto-ignition, flameless combustion, MILD combustion (moderate intense low-oxygen dilution), usually in burners, and (incongruously) homogeneous charge compression ignition, through zones of reactivity gradients [31]. In engines "mild" is normally used as a description of slight, but not intense, knock.

A range of different engine auto-ignition conditions were studied, covering four different engines, 1-4, all at different locations, operating in 10 modes, A to J, summarised in Table 1. The operational regime, in terms of auto-ignition and knock are shown, relative to the developing detonation peninsula boundary and contours of $\overline{E}\partial \ln T/\partial \overline{r}$, on Fig. 4.

The controlled auto-ignition regime is covered by Conditions A to C. The progression from this regime, through no knock to super-knock, is traced by the progressive blackening of the symbols on Fig. 4, indicative of strengthening developing detonations. Pressures and temperatures are given in Table 1. Condition D is representative of no knock, H represents slight knock, E heavier knock. Conditions F, G, I, and J represent super-knock, associated with auto-ignitive pre-ignition [38], and subsequent strong developing detonations.

For Conditions A to C, the Hydra single cylinder engine was the only engine operating entirely in the controlled auto-ignition regime, with ϕ = 0.25 [32]. The low value of ϕ, combined with flame extinctions due to the engine turbulence, inhibited deflagrative burning, in favour of auto-ignitive burning. In these, and all other cases considered here for the derived data on Fig. 4, it is assumed that r_o = 5 mm and $\partial T/\partial r$ = -2 K/mm. Primary reference fuels were employed with this engine, comprised of volumetric proportions of 0.84 *i*-octane and 0.16 *n*-heptane. Following [33] values of τ_i were obtained by multiplying the stoichiometric value at the relevant temperature in [11] by $0.8/\phi$,

with τ_i varying as $P^{-1.7}$ [6,32]. Values of τ_e were taken from [5] with the same allowances for ϕ and *P*. These enabled ξ, ε , and $\overline{E}$ to be evaluated [32]. The engine was free of knock and smooth-running, with minimal cyclic variations, for all three conditions. Figure 4 indicates, with reasonable accuracy, that the three operational points A to C are in the subsonic auto-ignition regime, with no deflagration. It suggests that condition B, was close to knock, a consequence of the low value of ξ at 811K, see Fig. 1. In the very early stages of knock, originating at a single hot spot, the amplitude of the pressure pulse is proportional to ξ^{-2} [38]. The low values of - $\overline{E}\left(\partial \ln T/\partial \overline{r}\right)$ tend to confirm that combustion was in the auto-ignitive mode. Spark-assisted compression ignition is sometimes used to control the initiation of deflagration when operating in the mixed auto-ignitive/deflagrative regime [29].

The second engine was spark-ignited, SI, multi-cylindered and turbo-charged, operating under the Conditions D, E, F [34] on Table 1. Here OI refers to the Octane Index, which is the Octane Number of the Primary Reference Fuel that just knocked under the same conditions. The test Conditions exhibited three gradations of developing knock, ranging respectively, from no discernible auto-ignition or knock, outside the peninsula, through fairly heavy knock, to pre-ignition followed by super-knock, within the toe of the peninsula, on Fig. 4. The mixtures became progressively more reactive, as a result of increasing temperatures and pressures. The third engine, at the single condition, G, [35] was similarly SI and turbo-charged, and had a similar fuel to the second engine, characterised respectively, by Octane Indices, OI, of 107 and 105. Values of τ_i and τ_e were taken to be the same as those of the surrogate fuel, the chemical kinetic scheme for which is described in [5]. These values enabled those of ξ, ε , and $\overline{E}$ to be found for the conditions for both engines. Super-knock occurred in the second engine for the condition F, and in the third engine for the single condition G.

The fourth engine, also turbo-charged, under the Conditions H, I, J, exhibited similar trends at high *P* and *T* [36,37] Super-knock usually occurs infrequently, and this aspect was studied carefully at Condition J. In an attempt to explain its spasmodic nature, temporal changes in pressure were recorded over 5,000 engine cycles. This captured a few rare records of super-knock [36]. From the engine pressure records in Fig. 7 of [39], it can be seen that super-knock was followed by an appreciably lower exhaust gas *T* and *P*. There was a consequently increased, air inhalation into the next cycle, and a lower temperature of recirculated burned gas. This lower *T* and *P* resulted in a reduced burn rate that, in turn, increased the exhaust *T* and *P*. Consequently, the burned gas recirculated into the third cycle would be at a higher temperature, possibly sufficient to induce auto-ignitive pre-ignition, particularly in the vicinity of the hot exhaust valve, Although pre-ignition does not necessarily cause super-knock, it was always a pre-condition for its occurrence [36]. Pre-ignition

is akin to spark advance and, because of the high turbulent burning velocities at the high T and P [40], these values would be rapidly increased still further to create vigorous auto-ignition and super-knock within the toe of the peninsula. This sequencing could explain the observed occurrence in this instance of super-knock every other cycle.

At the present time the details of the pre-ignition mechanism are unclear. One suggestion has been that fuel droplets from the injecting spray impinge on the cylinder wall and mix with lubricating oil and mixture droplets moving in to the gas phase [41,42]. Long-chain molecules from the lubricant with its additives are sufficiently auto-ignitive to create mild auto-ignitions that can, nevertheless, initiate a flame [39]. However, some evidence suggests that, at the observed temperatures and pressure of such hot spots, the mixture would have to be rather more auto-ignitive than heptane/air [39,43].

6. Origins of the hot spots

An estimate was made of the nature of an automotive hot spot generated through the dissipation of turbulent energy. The cascade of turbulent energy flux from the largest to the smallest length and time scales terminates in its complete dissipation as molecular motion, at the Kolmogorov scale of distance, η. This is reviewed in the context of combustion in [44]. If the mass specific rate of turbulent energy dissipation is ε_d, and the kinematic viscosity, v, then:

$$\eta = (v^3/\varepsilon_d)^{0.25}. \quad (13)$$

The Kolmogorov time scale is given by:

$$\tau_\eta = (v/\varepsilon_d)^{0.5}. \quad (14)$$

Power spectral densities [44] and spectra of vorticity fluctuations [45] have been measured in wind tunnels. Informative spatial vorticity contours have been obtained from direct numerical simulations [46]. Values of ε_d are found by integrating the 3D energy spectrum in terms of the resulting vorticity, ω, with:

$$\varepsilon_d = v\omega^2. \quad (15)$$

The rms strain rate was defined by Taylor [47], in terms of the Taylor scale of distance, λ, and the rms turbulent velocity, u' by:

$$u'/\lambda = (\varepsilon_d/v)^{0.5}15^{-0.5}. \quad (16)$$

From Eqs (14) and (15):

$$\tau_\eta = \omega^{-1}. \quad (17)$$

DNS of isotropic turbulence [46] show the creation of coherent, cylindrical, ribbon-like vortices, within which exist small regions of very high vorticity, of lifetime $< 0.3\ \tau_\eta$. These reside within a

background vorticity with lifetimes < τ_η. The former occupy 1%, and the latter 25%, of the total volume. Vortices with a lifetime < τ_η had a radius of about 4η. In turbulent flame analyses a limiting small scale radius of 6η has been employed [48].

The possibility of such vortices generating auto-ignitive hot spots, was estimated by assuming that the energy dissipated in a Kolmogorov scale vortex tube, during the Kolmogorov time, is equal to the enthalpy increase in the same volume. Hence, if the associated temperature increase is ΔT, and C_p is the mass specific heat at constant pressure, then, utilising Eq. (14),

$$\varepsilon_d \tau_\eta = (\varepsilon_d \nu)^{0.5} = c_p \, \Delta T. \qquad (18)$$

Normalised turbulent burning velocities and flame extinctions due to turbulence, can be correlated in terms of their Karlovitz stretch factor, K, and the strain rate Markstein numbers [40], with the turbulent Reynolds number, R_l, based upon the integral length scale. l, with

$$K = (u'/\lambda)(\nu/u_l^2) = 0.25(u'/u_l)^2 R_l^{-0.5}. \qquad (19)$$

From Eqs. (16) and (19):

$$(\varepsilon_d \nu)^{0.5} = (0.25 \text{x} 15^{0.5})(u'^{3/2})(\nu/l)^{0.5}. \qquad (20)$$

Consequently, a high energy dissipation is favoured by high values of u' and low values of l. Some typical engine conditions, under which hot spots might exist, are u' = 5 m/s, ν = 1.5 10^{-6} m^2/s, l = 2 mm, and c_p = 1250 J/kg/K. These values in Eqs. (20) and (18) yield the low value of ΔT = 0.00024K. With regard to the estimated size of the hot spot, following [48], with a vortex tube diameter of 12η, Eq. (13) gives a dissipative diameter of 33 μm.

For many conditions such a diameter would exceed the critical size of a hot spot that is necessary to initiate both an auto-ignition and a propagating flame [39]. However, the very small temperature elevation, due to turbulent energy dissipation, makes this an unlikely initiator of either phenomena. More likely triggers would appear to arise from the small scale turbulent mixing of the reactants with recirculated burned gas from the previous cycle, as discussed in Section 5, and heating from hot surfaces, such as exhaust valves. Also as discussed, pre-ignition might be enhanced at hot spots by fragments of lubricant of low τ_i. Although the consequential damage can be serious, pre-ignition and super-knock are both rare and random.

7. Conclusions

i. The ξ and ε coordinates of the detonation peninsula boundary have been shown to be applicable over a wide range of fuels.

ii. The $\overline{E}$ parameter in Eq. (11) enables contours of hot spot temperature elevations to be inserted on the ξ / ε diagram, as on Fig. 4.

iii. An approximate boundary, at which auto-ignitive burning becomes less probable than deflagrative flame propagation, has been identified on the ξ / ε diagram. Greater certainty of this requires knowledge of the turbulent combustion dimensionless groups and the conditions for turbulent flame extinction.

iv. The necessary localised temperature elevations at hot spots that are compatible with auto-ignition are unlikely to arise solely from the dissipation of turbulent energy.

v. The different regimes for hot spot auto-ignition, extending from controlled auto-ignition at one limit, through the development of knock to super-knock, can be identified through the values of τ_i, τ_e, and $\overline{E}$ on the ξ / ε diagram. More needs to be known about the detailed structure of the hot spots and their sizes.

vi. The use of the detonation peninsula to identify engine knock intensity, avoids some of the problems of attempting to assess fuels that are very different from *i*-octane/*n*-heptane, operating at pressures and temperatures very different from those in the RON and MON tests [32].

vii. The super-knock regime, identified on the ξ/ε peninsula, corresponds to that for strong, stable, continuous detonations in ducts. Both are characterised by values of ξ close to unity, with low values of $(\xi\varepsilon)$, $\overline{E}$, and hot spot temperature gradients [6]. These interrelationships are expressed by Eq. (11).

Memorial

Shortly before his death on 4th July following a heart attack, Norbert Peters approved the manuscript of this paper for submission to "Combustion and Flame". He is sorely missed by very many. Author DB collaborated with him over 35 years, including 14 when both were Editors of the Journal, At the ICDERS Colloquium in Leeds on the 5th August 2015 over 300 delegates paid tribute to Norbert at a Memorial Meeting.

Acknowledgements

Xin He is thanked for further information on the fuel for Engine 4, and Zheng Chen for further information on the work described in [8].

References

1. Ya.B. Zel'dovich, Regime classification of an exothermic reaction with nonuniform intial conditions, Combust. Flame 39: (1980) 211-214.

2. D. Bradley, C. Morley, X.J. Gu XJ, D.R. Emerson, Amplified pressure waves during autoignition: relevance to CAI engines, Proc. SAE Powertrain & Fluid Systems Conf. and Exhibition, San Diego, CA, 21–24 October (2002). Warrendale, PA: Society of Automotive Engineers.

3. X.J. Gu, D.R. Emerson, D. Bradley, Modes of reaction front propagation from hot spots, Combust. Flame 133 (2003) 63-74.

4. A.E. Lutz, R.J. Kee, J.A. Miller, H.A. Dwyer, A.K. Oppenheim, Dynamic effects of autoignition centers for hydrogen and C1, 2-hydrocarbon fuels, Proc. Combust. Inst. 22 (1988) 1683–1693.

5. G.T. Kalghatgi, D. Bradley, J. Andrae, A.J. Harrison, The nature of 'superknock' and its origins in SI engines. Internal Combustion Engines: Performance, Fuel Economy and Emissions, IMechE London, UK, 8-9 December, Institution of Mechanical Engineers (2009).

6. D. Bradley, Autoignitions and detonations in engines and ducts, Phil. Trans. Royal Soc. A 370 (2012) 689-714**.**

7. J. Rudloff, J.M. Zaccardi, S. Richard, J.M. Anderlohr, Analysis of preignition in highly charged SI engines: emphasis on the auto-ignition mode, Proc. Combust. Inst.34 (2013) 2959-2967.

8. Peng Dai, Zheng Chen, Shiyi Chen, Yiguang Ju, Numerical experiments on reaction front propagation in *n*-heptane/air/mixture with temperature gradient, Proc. Combust Inst. 35 (2014) 3045–3052.

9. N. Peters, B. Kerschens, G. Paczko, Super-knock prediction using a refined theory of turbulence, (2013), SAE paper 2013-01-1109.

10. G.T. Kalghatgi, Developments in internal combustion engines and implications for combustion science and future transport fuels, Proc. Combust. Inst. 35 (2015) 101-115.

11. K. Fieweger, R. Blumenthal, G. Adomeit, Self-ignition of S.I. engine model fuels:

a shock tube investigation at high pressure, Combust. Flame 109 (1997) 599-619.

12. C. Morley, Gaseq Chemical Equilibrium Program. c.morley@ukgateway.net

13. Longting He, P. Clavin, Theoretical and numerical analysis of the photochemical initiation of detonations in hydrogen-oxygen mixtures, Proc. Combust. Inst. 25 (1994) 45-51.

14. V.N. Voevodsky, R.I. Soloukhin, On the mechanism and explosion limits of hydrogen-oxygen chain self ignition in shock waves, Proc. Combust. Inst. 10 (1965) 279-283.

15. J.W. Meyer, A.K. Oppenheim, On the shock-induced ignition of explosive gases, Proc. Combust. Inst 13 (1971) 1153-1164.

16. M.I. Radulescu, H.D. Ng, J.H.S, Lee, B. Varatharajan, The effect of argon dilution on the stability of acetylene/oxygen detonations, Proc. Combust. Inst. 29, (2002) 2825–2831.

17. M. Short, G.J. Sharpe, Pulsating instability of detonations with a two-step chain-branching reaction model: theory and numeric, Combust. Theory Modell. 7 (2003) 401–416.

18. M.I. Radulescu, G.J. Sharpe, C.K. Law, J.H.S. Lee, The hydrodynamic structure of unstable cellular detonations, J.Fluid Mech. 580 (2007) 31–81.

19. J.E. Shepherd, Detonation in gases, Proc. Combust. Inst. 32 (2009) 83–98.

20. M.I. Radulescu, G.J. Sharpe, D. Bradley, A universal parameter for quantifying explosion hazards, detonability and hot spot formation, the χ number, Proceedings of the Seventh International Seminar on Fire and Explosion Hazards,(2013) pp. 617-626, Research Publishing, Singapore. Eds. Bradley D, Makhviladze G, Molkov V, Sunderland P, Tamanini F.

21. Honghui Teng, Hoi Dick Ng, Kang Li, Changtong Luo, Zonglin Jiang, Evolution of cellular structures on oblique detonation surfaces, Combust. Flame 162 (2015) 470-477.

22. D. Bradley, M. Lawes, M.S. Mansour, Correlation of turbulent burning velocities of ethanol–air, measured in a fan-stirred bomb up to 1.2 MPa, Combust. Flame 158 (2011) 123–138.

23. R. Sankaran, Hong G. Im, E.R. Hawkes, J.H. Chen, The effect of non-uniform temperature distribution on the ignition of a lean homogeneous hydrogen-air mixture, Proc. Combust. Inst. 30 (2005) 875-882.

24. S.M. Walton, X. He, B.T. Zigler, M.S. Wooldridge, A. Atreya, An experimental investigation of iso-octane ignition phenomena, Combust. Flame 150 (2007) 246-262.

25. A.B. Mansfield, M.S. Wooldridge, High-pressure low-temperature ignition behavior of syngas mixtures, Combust. Flame 161 (2014) 2242-2251.

26. Y. Minamoto, N. Swaminathan, S.R. Cant, T. Leung, Morphological and statistical features of reaction zones in MILD premixed combustion, Combust. Flame 161 (2014) 2801-2814.

27. R.G. Abdel-Gayed, D. Bradley, F.K.K. Lung, Combustion regimes and the straining of turbulent premixed flames, Combust. Flame 76 (1989) 213-218.

28. D. Bradley, M. Lawes, Kexin Liu, R. Woolley, The quenching of premixed turbulent flames of iso-octane, methane and hydrogen at high pressures, Combust. Inst. 31 (2007) 1393-1400.

29. Dai, S.G. Russ, N. Trigui, K.V. Tallio, Regimes of premixed turbulent combustion and misfire modeling in SI engines, (1998) SAE paper 982611.

30. A. Robert, S. Richard, O. Colin, T. Poinsot, LES study of deflagration to detonation mechanisms in a down sized spark ignition engine, Combust. Flame 162 (2015) 2788-2807.

31. *Lean Combustion: Technology and Control* Ed. Derek Dunn-Rankin, Elsevier, (2008).

32. D. Bradley, R.A. Head, Engine autoignition: the relationship between octane number and autoignition delay time, Combust. Flame 147 (2006) 171-184.

33. D. Bradley, C. Morley, H.L. Walmsley, Relevance of Research and Motor Octane numbers to the prediction of engine autoignition, Proc. SAE Fuels and Lubricants Meeting, Toulouse. (2004) SAE paper 2004-01-1970, Book No. SP-1884, "Homogeneous Charge Compression Ignition (HCCI)".

34. P. Rothenberger, GM Powertrain, Germany, Private Communication [6].

35. P.W. Manz, VW Germany Private Communication [6].

36. Zhi Wang,, Hui. Liu, Tao Song, Yunliang Qi, Xin He, Shijin. Shuai, JianXin Wang, Relationship between super-knock and pre-ignition, Int. J. Engine Research. 16 (2015) 166-180.

37. Z. Wang, Hui Liu, T. Song, Y. Xu, J.X. Wang, Investigation on Pre- ignition and Super-Knock in Highly Boosted Gasoline Direct Injection Engines, (2014), SAE paper 2014-01-1212.

38. D. Bradley, G.T. Kalghatgi, Influence of autoignition delay time characteristics of different fuels on pressure waves and knock in reciprocating engines, Combust. Flame 156 (2009) 2307-2318.

39. G.T. Kalghatgi, D. Bradley, Pre-ignition and 'super-knock' in turbocharged spark-ignition engines, Int. J of Engine Research 12(4) (2012) 399-414.

40. D. Bradley, M. Lawes, K. Liu, M.S. Mansour, Measurements and correlations of turbulent burning velocities over wide ranges of fuels and elevated pressures, Proc. Combust. Inst. 34 (2013) 1519–1526.

41. A. Zadeh, P. Rothenberger, W. Nguyen, et al., Fundamental approach to investigate pre-ignition in boosted engines, (2011), SAE paper 32011-01-0340.

42. C. Dahnz, K.H. Han, U. Spicher, et al., Investigation on pre-ignition in highly supercharged engines, (2010), SAE paper 2010-01-0355.

43. N. Peters, G. Paczko, .H. Pitsch, Wall Film Evaporation causing Pre-ignition in Turbocharged Gasoline Engines, 25th International Colloquium on the Dynamics of Explosions and Reactive Systems Leeds, UK, (2015).

44. D. Bradley, "How fast can we burn?", Proc. Combust. Inst. 24 (1992) 247-262.

45. Y. Zhu, R.A. Antonia, On the correlation between enstrophy and energy dissipation rate in a turbulent wake, Applied Scientific Research 57 (1997) 337-347.

46. J. Jiménez, A.A. Wray , P.G. Saffman, R.S.Rogallo,The structure of intense vorticity in isotropic turbulence, J. Fluid Mech.255 (1993) 65-90.

47. G.I. Taylor, Statistical theory of turbulence – II, Proc. Roy. Soc. Lond. A151 (1935) 444-454.

48. H. Kobayashi, T. Tamura, K. Maruta, T. Niioka, F.A. Williams, Burning velocity of turbulent premixed flames in a high pressure environment, Proc. Combust. Inst. 26 (1996) 389-396.

Figure and Table Captions

Figure 1. Computed values of ξ for five different Octane Numbers of Primary Reference Fuels at 4 MPa and $\partial T/\partial r$ = -2 K/mm. Data from [11].

Figure 2. History of a hot spot, r_o = 3 mm, with ξ = 1, stoichiometric 0.5 H_2/0.5 CO/air, T_o= 1200K and P_o=5.066 MPa, τ_i = 39.16 μs. Time sequence (μs) 1-35.81, 2-36.16, -36.64, 4-37.43, 5-37.72, 6-38.32, 7-38.86, 8-39.13. (a) temperature, (b) pressure, (c) combustion wave speed.

Figure 3. ξ/ε regime diagram, for hot spot auto-ignition, showing the detonation peninsula and other regimes. Symbols indicate data from different fuels. ◯: H_2/CO/air [4], □: *n*-C_7H_{16}/air, Δ: *i*-C_8H_{18}/air.

Figure 4. Increasing black fill of the symbols indicates increasing severity of knock for the different conditions in Table 1, from no knock, through mild knock. to super-knock.

Table 1. Engine auto-ignition and super-knock conditions.

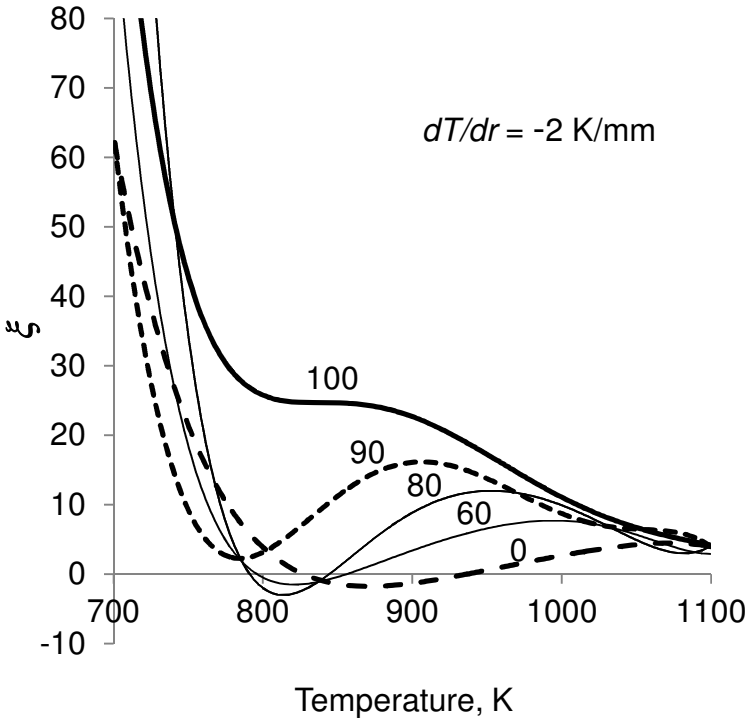

Figure 1. Computed values of ξ for five different Octane Numbers of Primary Reference Fuels at 4 MPa and $\partial T/\partial r$ = -2 K/mm. Data from [11].

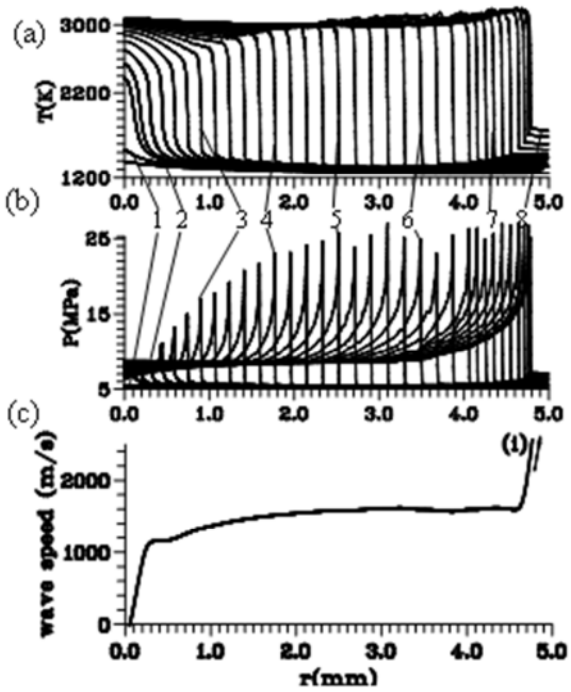

Figure 2. History of a hot spot, r_o = 3 mm, with ξ = 1, stoichiometric 0.5 H_2/0.5 CO/air, T_o= 1200K and P_o=5.066 MPa, τ_i = 39.16 μs. Time sequence (μs) 1-35.81, 2-36.16, -36.64, 4-37.43, 5-37.72, 6-38.32, 7-38.86, 8-39.13. (a) temperature, (b) pressure, (c) combustion wave speed.

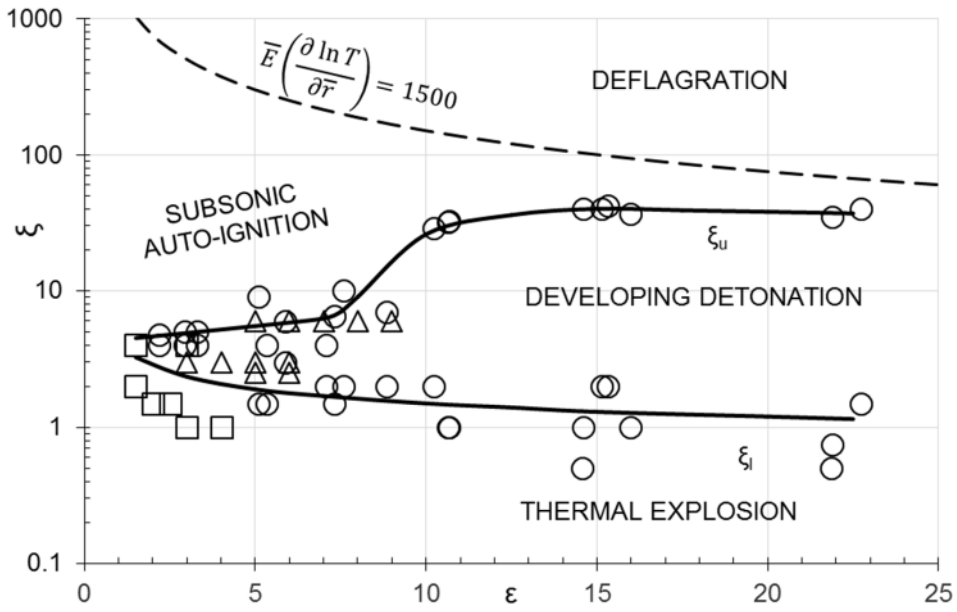

Figure 3. ξ/ε regime diagram, for hot spot auto-ignition, showing the detonation peninsula and other regimes. Symbols indicate data from different fuels ◯: H_2/CO/air [4], □: n-C_7H_{16} /air, Δ: i-C_8H_{18}/air.

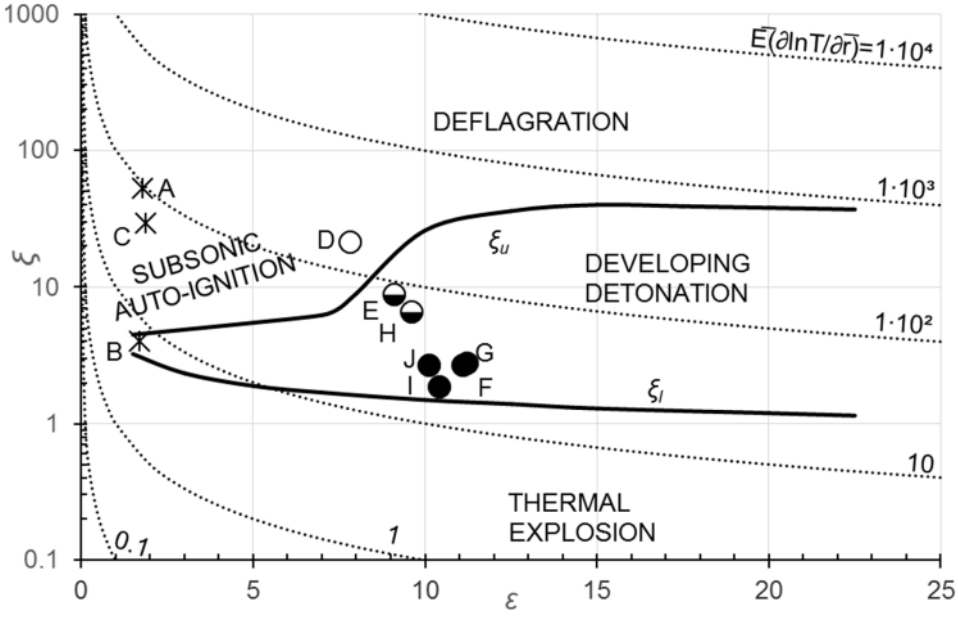

Figure 4. Increasing black fill of the symbols indicates increasing severity of knock for the different conditions in Table 1, from no knock, through mild knock. to super-knock.

Table 1. Engine auto-ignition and super-knock conditions.

Engine	Fuel	Auto-ignitive mode	Fig. Ref.	φ	T K	P MPa	$\overline{E}$	Ref.
1. Hydra single cylinder with Roots blower. (Shell Global Solutions).	PRF 84 [5,11,33]	Controlled benign auto-ignition.	A	0.25	729	6.52	6,799	[32,6]
			B	0.25	811	4.84	543	
			C	0.25	1057	3.37	5,829	
2. Turbo-charged S.I. engine (GM Powertrain)	RON/MON 95/85, OI=105. Surrogate 0.62 *i*-octane, 0.29, toluene, 0.09 *n*-heptane, OI=105 [5]	No auto-ignition	D	1.0	800	7.0	13,269	[34]
		Fairly heavy knock	E	1.0	850	9.0	6,716	[34]
		Pre-ignition, super-knock	F	1.0	926	12.8	2,696	[34]
3. Turbo-charged S.I. engine (VW)	RON/MON 98/89, OI=107. Surrogate as above [5]	Pre-ignition, Super-knock	G	1.0	918	13.3	2,822	[35]
4. Turbo-charged S.I. engine (Tsinghua University, Beijing)	Composition in [37]. RON/MON, 94.1/81.9. Data for 93.4/81 from [5,32].	Slight knock	H	1.0	824	10.45	5,229	[36,37]
		Super-knock, deflagration	I	1.0	949	10.91	1,906	[36,37]
		Super-knock, detonation	J	1.0	917	10.5	2,467	[36,37]